A New Pulse Magnet for the RCS Injection Shift Bump Magnet at J-PARC

T. Takayanagi, K. Yamamoto, J. Kamiya, P. K. Saha, T. Ueno, K. Horino, M. Kinsho, and Y. Irie

***Abstract*—The 3-GeV rapid-cycling synchrotron at the Japan Proton Accelerator Research Complex has achieved the high-power beam operation equivalent to 1 MW. As a next step, a study of an upgrade is in progress to mitigate the dose exposure of the maintenance workers in a high residual dose environment and realize the further high intensity beam power. Regarding the upgrade plan's provisions for radiation protection, a new injection scheme has been proposed to make space available for radiation shielding. The total length of the two shift bump magnets of the four magnets is reduced for this purpose, while the other two magnets in the injection straight section remain unchanged. As a result, the two types of pulse magnets are connected separately in series and are excited by two independent power supplies, which are made possible by splitting the presently installed power supply. A structural analysis of the new shift bump magnet is in progress, including simulations of the effects of eddy currents and the coil temperatures by OPERA-3D. This paper describes preliminary results of this analysis and the outlines the modified power supply design.**

***Index Terms*—Accelerator magnets, eddy currents, electromagnetic analysis, magnetic field measurement, pulsed power supplies.**

I. Introduction

JAPAN Proton Accelerator Research Complex (J-PARC) [1] consists of three proton accelerators: a 400-MeV linear accelerator (LINAC), a 3-GeV rapid-cycling synchrotron (RCS) [2], and a 50-GeV main ring (MR). The H^- beam from the LINAC is multi-turn charge-exchange injected into the RCS through a thin carbon foil. The injected protons stripped by the foil are accelerated up to 3 GeV at a repetition rate of 25 Hz and aims at the output of 1 MW.

In January 10, 2015, the RCS demonstrated the acceleration of a high-power beam equivalent to 1 MW. Then, a beam study aiming at 1 MW continuous operation was performed. After a study at 400 kW beam power operation, a residual dose of 15 mSv/h around the 1st foil of the RCS injection area was confirmed [3]. Therefore, a test operation for the beam loss reduction [4], [5] was performed and the residual dose was reduced to 9 mSv/h [6]. However, only this reduction is not sufficient for safely performing maintenance work in this area. In addition, the radio-activation of the injection area will become an issue in future to achieve the 1 MW continuous operation and further high-power beam operation. Therefore, we have designed a new injection scheme that will reduce dose exposure during maintenance work around the beam injection area.

Manuscript received September 1, 2017; accepted December 11, 2017. Date of publication December 22, 2017; date of current version January 10, 2018. *(Corresponding author: T. Takayanagi.)*

T. Takayanagi, K. Yamamoto, J. Kamiya, P. K. Saha, T. Ueno, K. Horino, and M. Kinsho are with the J-PARC Accelerator Division, Japan Atomic Energy Agency, Tokai 319–1195, Japan (e-mail: tomohi-ro.takayanagi@j-parc.jp).

Y. Irie is with KEK, Tsukuba 305–0801, Japan.

Color versions of one or more of the figures in this paper are available online at http://ieeexplore.ieee.org.

Digital Object Identifier 10.1109/TASC.2017.2786285

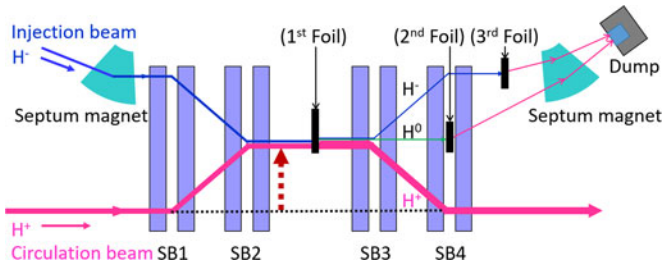

Fig. 1. Outline of the injection system.

II. Injection System

A. Present System

An outline of the present RCS injection system [7] is shown in Fig. 1. An H^- beam from the LINAC passes through the thin carbon foil that strips electrons and resulting H^+ beam merges with the circulating beam. On the other hand, unstripped particles are converted to protons by the second foil and the third foil and they are transported to the beam dump by a septum magnet.

The yoke of the presently installed shift bump (SB) magnet [8] is separated at the center to make space for the second foil. Moreover, the four SB magnets have the same shape and are connected in series so that they can be excited with a single power supply [7]. With this system, the beam transformed by the second foil can efficiently be guided to the dump line. It is also possible to generate a fixed injection trajectory without any timing jitter or level fluctuations between the four magnets. The injection orbit produced by the four SB magnets is also fixed by the flat top of the trapezoidal waveform of the pulsed power supply. To maintain a stable injection orbit, a low-noise waveform with a very flat top is necessary. To satisfy this requirement, a commutation method using a capacitor was adopted [9], which suppressed current ripple noise that arises from the switching involved in forming the waveform [10].

B. New Injection Scheme

An investigation of the cause of this high activation found that the interaction of the injection and circulation beam with

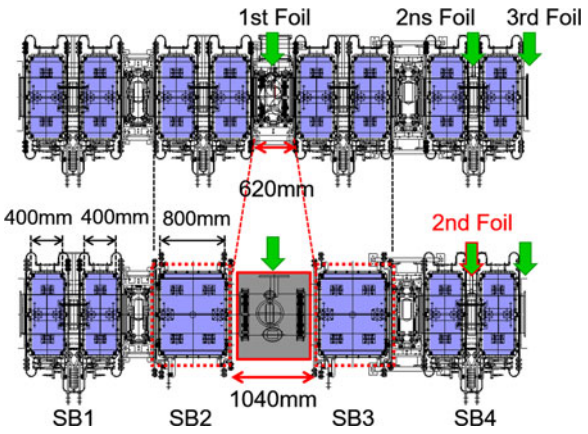

Fig. 2. New design concept: (Upper) present layout. (Lower) New layout.

TABLE I
PRESENT AND NEW DESIGN PARAMETERS OF THE SHIFT BUMP MAGNET

Contents	Present design	New design
Number of magnets	4	4
Yoke type	Split	Split and integrated
Connection type	4 units in series	2 units in series
Number of power supplies	1	2
Rated value	32 kA/12 kV	16 kA/12 kV

the first foil could explained most of the problem [11]. To reduce the radiation exposure of maintenance workers near the injection area, we considered covering the area with a high radiation dose by a radiation shield. However, the present straight injection section leaves no spaces to install shielding. Therefore, we have reconfigured the space by jointing the split yokes of the SB2 and SB3 magnets located upstream and downstream of the first foil. Even with this new injection scheme, the positions of the second and third foils must be left unchanged.

To solve these problems, only the SB2 and SB3 magnets were changed to joined yokes, and SB1 and SB4 magnets retain the present split yoke, as shown in Fig. 2. The residual dose of 10 mSv/h should be reduced to 100 μSv/h by 200 mm thick iron shielding (K. Yamamoto calculated). The design parameters of the presently installed and new SB magnets are provided in Table I. The two kinds of SB magnets will each be connected separately in series and will be excited by independent power supplies, which will be made by splitting the presently installed power supply.

III. APPLICATION DESIGN AND ANALYSIS

A. Design of the New SB Magnet

The split yoke of the present SB magnet is configured as one magnetic pole [8]. The coil has two turns, and the low inductance allows the magnet to excite a high-speed pulse. On the other hand, the yoke of the new SB magnet has a joined configuration, which maintains the same core length of 800 mm as the total length of the split yokes is 400 mm $\times$ 2. When the current rating of the power supply is halved by forming the two independent supplies, the number of turns of the coil is doubled to conserve the magnetic field.

Since the skin effect significantly affects fast excitation waveforms, a copper plate with a large surface area is used for the coil. Further, the area of the copper plate contacting the air is increased, thereby improving the cooling efficiency. This coil structure design is the same for both the present and new SB magnets.

In the present SB magnet, the cooling water piping cracks and leaks frequently. This maintenance issue frequently halts accelerator operation for a long time, and the leaked cooling water also presents a risk for radiation exposure to the workers performing replacement work. Therefore, for the new SB magnet design, we will consider a change from water cooling to forced air cooling.

B. OPERA-3D Modules

The previously designed SB magnet with the split magnetic field distribution was analyzed only using OPERA-2D analysis and OPERA-3D's TOSCA module. OPERA-2D solves for time invariant magnetic or electric fields. The base design was examined in OPERA-2D. TOSCA solves nonlinear magnetostatic equations in three dimensions. The structure realizing good magnetic field distribution was performed by TOSCA.

OPERA-3D's ELEKTRA module analyzes the time-dependent electromagnetic field and takes the effects of eddy currents into account. Using OPERA with version 16 or later, it is possible to analyze an eddy current of the coil by dividing a mesh with the finite element method in the magnet coil in addition to the previous ability to analyze eddy currents in the iron core. Moreover, the TEMPO module analyzes transient and steady-state thermal fields caused by electromagnetic heating and external heat sources. TEMPO calculates heat sources using numerical results including eddy current effects delivered by the ELEKTRA module. We have compared these simulation tools in the OPERA-3D modules (TOSCA, ELEKTRA, TEMPO) with measurement results on the present SB magnets.

IV. EVALUATION OF THE RESULT OF THE MEASUREMENT AND ANALYSIS FOR DESIGN OF NEW SB MAGNET

A. Evaluation of Magnetic Field Distribution

The result of measurements and analysis (TOSCA, ELEKTRA) on the present SB magnet are shown for comparison in Fig. 3, and a picture of the analysis model in ELEKTRA is shown in Fig. 4. The SB magnet repeatedly outputs a magnetic field of trapezoidal form with 500 μs rise-time, 650 μs flat-top, and 500 μs fall-time at 25 Hz. In Fig. 3, numerical results show that beam injection begins 150 μs after the start of the flat top. The magnetic field distribution of numerical results from ELEKTRA agrees very well with the measured values. On the other hand, the measurement results were different from the values simulated by TOSCA. The measurement results for the magnetic field distribution using the search coil were performed after the SB magnets were fabricated [12]. We consider that the eddy current at the end plate and the coil explains this

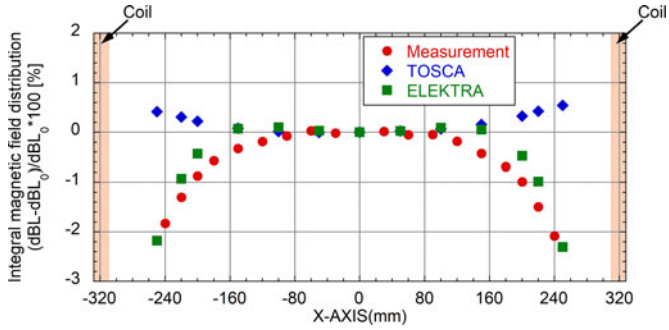

Fig. 3. Result with comparison of the results of measurement and analysis (TOSCA, ELEKTRA) using the present SB.

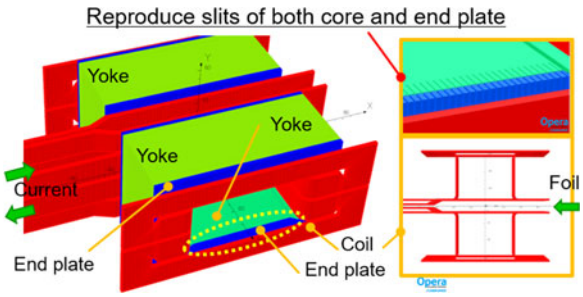

Fig. 4. Analysis model of the present SB magnet of ELEKTRA.

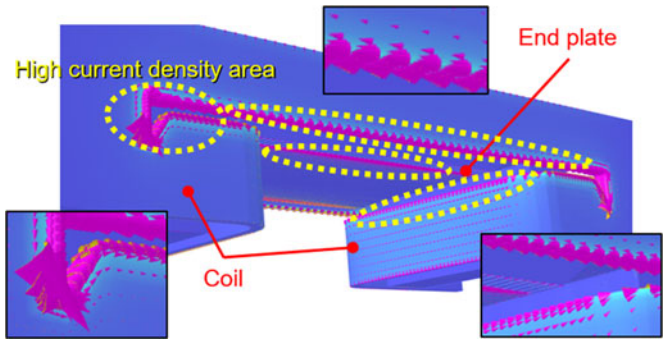

Fig. 5. Analysis result of the distribution of the eddy current density at the end plate and the coil.

discrepancy, as illustrated in Fig. 5. The arrow in Fig. 5 marks the vector potential of the eddy current. This result shows that the current does not flow evenly in the copper plate of the SB magnet coil but takes the shortest path along the edge.

B. Evaluation of Temperature

The temperature analysis module of TEMPO was evaluated using the temperature measurements from the coil of the present SB magnet. A picture of the magnet and the results are shown in Fig. 6. The cooling water was temporarily stopped, and then the temperature of the coil was measured. The temperature difference above and below the duct was 30 °C (140 °C and 112 °C, respectively). This difference at the upper and lower positions is explained by the relative positions of the air flows and the existence of the beam duct.

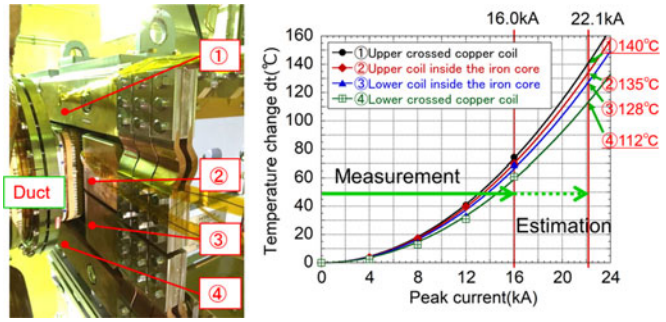

Fig. 6. (Left) Picture of the temperature measurement point of the present SB. (Right) Temperature of measurement result and estimated value.

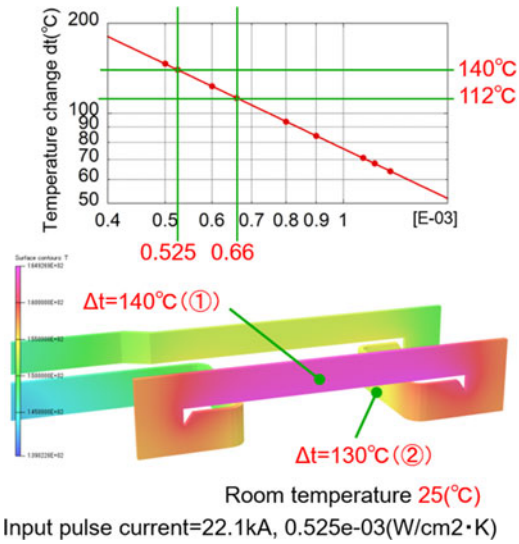

Fig. 7. (Upper) Heat transfer coefficient value corresponding to different temperature depending on installation position. (Lower) Analyses result of the coil temperature of the present SB magnet.

The heat transfer coefficient values at each position were calculated from the comparison with the temperature measurements in the presently installed area and the temperature of the coil was then analyzed. These results are shown in Fig. 7. The results of this temperature analysis showed a good agreement.

C. Analysis Result of New SB Magnet Model

Because of the good agreement between calculations and measurements, we designed a new SB magnet with a joined yoke has been performed using the ELEKTRA module. The model and numerical results for the integrated magnetic field are shown in Figs. 8 and 9, respectively. The exciting waveform for the simulation is that currently used in the accelerator utilization operation: 400 μs rise-time, 650 μs flat-top, and 350 μs fall-time. The numerical result corresponds to the timing before the beam injection. The homogeneity of the field distribution nearly matched the expected distribution. Further improvement of the magnetic field distribution is possible by optimizing the coil shape.

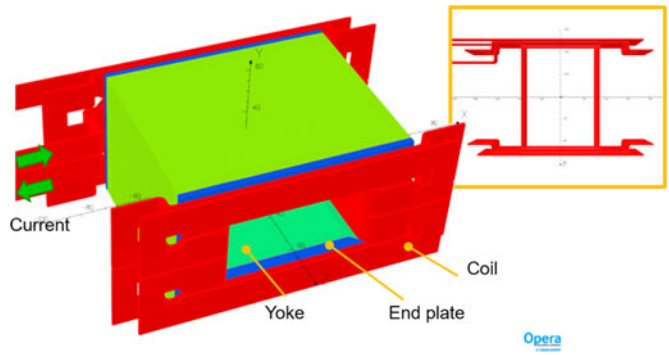

Fig. 8. Analysis model of the new SB magnet of ELEKTRA.

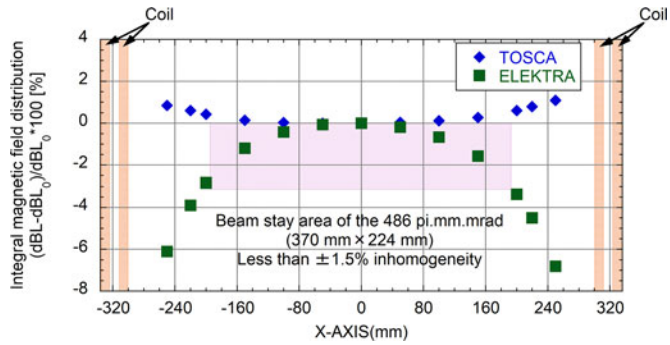

Fig. 9. Analysis results of the new SB magnet by TOSCA and ELEKTRA.

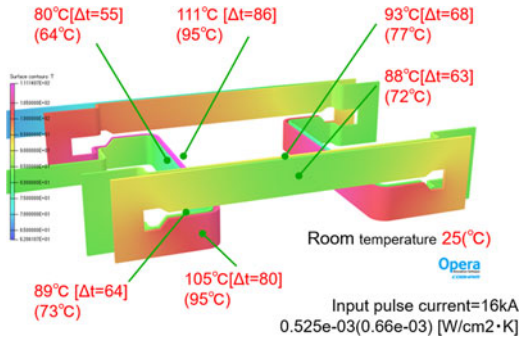

Fig. 10. Analyses result of the coil temperature of the new SB magnet.

The numerical results for the temperature is shown in Fig. 10. The temperatures calculated using two heat transfer coefficients are acceptable. The simulation was calculated for each transfer coefficient at all positions of the coil. The bracketed values are values for the alternate heat transfer coefficient. However, by taking the thermal interference with peripheral equipment, we could also consider a forced air-cooling system using fans in future design iterations.

V. Power Supply

A. Present Design

To obtain a stable orbit, high flatness and low noise are required for the exciting waveform. The power supply of the SB magnet was upgraded from the insulated gated bipolar transistor chopping system [10] to the capacitor commutation method system using the charging and discharging [9], [13]. This system produces the trapezoid waveform at 25 Hz repetition with only three times of switching per pulse. In the chopping system, noise due to switching occurs constantly during waveform formation. The commutation system suppresses ripple noise by limiting the number of switching. Therefore, the ripple noise caused by the continuous switching can be reduced considerably for the presently installed power supply.

B. Future Plan

To prepare the two independent power supplies after remodeling the present SB magnets, the presently installed power supply will be divided. The presently installed SB power supply is comprised of the 16 banks connected in parallel. Each bank includes 12 rise-fall units (Rf-unit) and 2 flat-top units (Ft-unit), and produces an output current of 2 kA and an output voltage of 12 kV. So, the maximum output current and output voltage of the whole array are 32 kA and 12 kV, respectively. In the future, eight banks will be operated as one power supply, and the maximum output current and output voltage will be 16 kA and 12 kV, respectively. To compensate for the halving of the power supply and to conserve the necessary magnetic field, the number of turns of the coil will be doubled for all the SB magnets.

The inductance per electromagnet will then be quadrupled, but the number of electromagnets connected in series is halved. In addition, since the rise and fall times of the bump waveform maintain the present specifications, the slope of di/dt of the excitation waveform is halved. As a result, the output per bank required by the new power supply system will be the same as the presently installed system. Therefore, the present banks can be used without any modifications.

However, to form a fixed injection orbit without fluctuations in the excitation timing between the two power supply units, a control system that adjusts the excitation timing between the two power supplies with 0.1 microsecond accuracy will be necessary.

VI. Conclusion

Design of a new injection scheme which allows sufficient shielding space and mitigates the radiation exposure of the maintenance workers has begun. To maintain the proven injection system with the required design modifications, a new design for the pulse magnets and modification of the power supply were verified. A new design is proposed in which the yoke of the presently installed SB is modified. From measurements of the magnetic field and temperature of the present electromagnets, we demonstrated that the ELEKTRA module in OPERA-3D is suitable for design work on these improvements. Further improvements of the magnetic field distribution of the new SB magnets is possible by optimizing the coil shape. Furthermore, since the number of turns of the present SB coil must also be doubled while conserving the split yoke, we plan to perform electromagnet analysis in future work.

REFERENCES

[1] [Online]. Available: https://j-parc.jp/index-e.html

[2] M. Kinsho, "Status of the J-PARC 3 GeV RCS," in *Proc. Int. Part. Accel. Conf. 2015*, pp. 3798–3800.

[3] K. Yamamoto *et al.*, "New injection scheme of J-PARC rapid cycling synchrotron." in *Proc. Int. Part. Accel. Conf. 2017*, pp. 579–581.

[4] H. Hotchi *et al.*, "Beam loss caused by edge focusing of injection bump magnets and its mitigation in the 3-GeV rapid cycling synchrotron of the Japan proton accelerator research complex," *Phys. Rev. Accel. Beams*, vol. 19, Jan. 2016, Art. no. 010401.

[5] H. Hotchi *et al.*, "Realizing a high-intensity low-emittance beam in the J-PARC 3-GeV RCS," in *Proc. Int. Part. Accel. Conf. 2017*, pp. 2470–2473.

[6] K. Yamamoto, "Worker dose under high-power operation of the J-PARC 3 GeV rapid cycling synchrotron," in *Proc. Int. Conf. Radiation Shielding and 19th Top. Meeting Radiation Protection Shielding Div. Amer. Nucl. Soc.*, 2016, Art. no. 07022.

[7] T. Takayanagi *et al.*, "Design of the injection bump system of the 3-GeV RCS in J-PARC," *IEEE Trans. Appl. Supercond.*, vol. 16, no. 2, pp. 1358–1361, Jun. 2006.

[8] T. Takayanagi *et al.*, "Design of the shift bump magnets for the beam injection of the 3-GeV RCS in J-PARC," *IEEE Trans. Appl. Supercond.*, vol. 16, no. 2, pp. 1366–1369, Jun. 2006.

[9] T. Takayanagi *et al.*, "Design and preliminary performance of the new injection shift bump power supply at the J-PARC 3-GeV RCS," *IEEE Trans. Appl. Supercond.*, vol. 24, no. 3, Jun. 2014, Art. no. 0503504.

[10] T. Takayanagi *et al.*, "Comparison of the pulsed power supply systems using the PFN switching capacitor method and the IGBT chopping method for the J-PARC 3-GeV RCS injection system," *IEEE Trans. Appl. Supercond.*, vol. 24, no. 3, Jun. 2014, Art. no. 3800905.

[11] M. Yoshimoto, H. Hotchi, S. Kato, K. Okabe, K. Yamamoto, and M. Kinsho, "Radio-activation caused by secondary particles due to nuclear reactions at the stripper foil in the J-PARC RCS," in *Proc. Int. Part. Accel. Conf. 2017*, pp. 2300–2302.

[12] T. Takayanagi *et al.*, "Improvement of the shift bump magnetic field for a closed bump orbit of the 3-GeV RCS in J-PARC," *IEEE Trans. Appl. Supercond.*, vol. 18, no. 2, pp. 306–309, Jun. 2008.

[13] T. Takayanagi, N. Hayashi, T. Ueno, K. Horino, K. Okabe, and K. Kinsho, "New injection bump power supply of the J-PARC RCS," in *Proc. Int. Part. Accel. Conf. 2015*, pp. 2908–2910.